Undergraduate Journal of Experimental Microbiology and Immunology (UJEMI) Vol. 29:1-10

Morphological and functional characterization of the C-terminal two-thirds of the autotransporter Ag43 alpha domain via site-directed mutagenesis in *Escherichia coli* DH5α

Alix Najera Mazariegos, Keegan McDonald, Max Tepes, Sarah Zhang

Department of Microbiology and Immunology, University of British Columbia, Vancouver, British Columbia, Canada

SUMMARY The role of Antigen 43 in bacterial aggregation and biofilm formation has been extensively studied, emphasizing its significance in bacterial resilience, antibiotic resistance, and infection persistence. Despite this knowledge, the specific influence and function of the alpha domain of Antigen 43 on bacterial colony morphology remains a poorly understood aspect. Antigen 43 is composed of an N-terminal signal sequence, alpha domain, autotransporter, and C-terminal beta domain. In this investigation, we employed site-directed mutagenesis to precisely delete the C-terminal two-thirds of the alpha domain of Antigen 43 in *Escherichia coli* DH5α cells. We aimed to obtain a more nuanced understanding of the specific regions of the alpha domain responsible for aggregation and the characteristic 'frizzy' colony morphology. While our results indicate the deletion of amino acids 193-551 did not eliminate aggregation, we surprisingly observed a modified aggregative behavior and altered colony morphology. Further validation through Western blot analysis and whole plasmid sequencing confirmed the deletion while also underscoring differences in Ag43 expression in the mutant bacteria. In summary, our study provides insights into the relationship between the alpha domain of Ag43 and bacterial behavior, suggesting that specific deletions within Ag43 may not entirely disrupt the aggregation process but rather modify it, prompting further exploration into the functional consequences of such deletions.

INTRODUCTION

Gram-negative bacteria employ a type Va secretion system known as classical autotransporters (AT) that play a critical role in virulence, adhesion, and biofilm formation (1). One such versatile autotransporter is Antigen 43 (Ag43). Encoded by *agn43*, this protein is expressed by both commensal and pathogenic *Escherichia coli* strains (2). Notably, it plays a crucial role in self-adhesion and has been linked to the aggregation and sedimentation of *E. coli* cells in liquid cultures (3). Expression of adhesins, particularly in strains expressing *agn43*, is closely associated with the initiation of urinary tract infections (UTIs). Furthermore, Ag43 significantly contributes to biofilm formation and colony morphology, yet the precise mechanism underlying its distinctive frizzy colony morphology remains unclear.

In clinical settings, the macroscopic characteristics of bacterial colonies, such as color, size, and texture, serve as valuable tools for profiling bacteria and identifying virulence factors or antibiotic resistance determinants. Previous research has demonstrated a correlation between *E. coli* colony morphology and antibiotic resistance in UTIs, highlighting the diagnostic potential of morphological phenotypes (4). Consequently, this project aims to investigate and elucidate the specific region within Ag43 that influences colony morphology.

Ag43 is made up of an N-terminal signal sequence, alpha domain (passenger domain), autotransporter, and C-terminal beta-barrel (3). The alpha domain of Ag43 (α43) folds into a right-handed three-stranded β-helix, forming an L-shaped protein with a twisted, irregular structure. This conformation, along with intricate networks of hydrogen bonds, contributes to the protein's aggregation function (5). The proposed universal mechanism suggests that interacting bacterial surfaces, covered with hook-like AT structures like Ag43, can self-assemble via a "handshake" mechanism to form aggregated communities. Building on these

Published Online: September 2024

Citation: Najera Mazariegos, McDonald, Tepes, Zhang. 2024. Morphological and functional characterization of the C-terminal two-thirds of the autotransporter Ag43 alpha domain via site-directed mutagenesis in *Escherichia coli* DH5α. UJEMI 29:1-10

Editor: Shruti Sandilya and Ronja Kothe, University of British Columbia

Address correspondence to: https://jemi.microbiology.ubc.ca/

insights, our study aims to unravel the specific region within Ag43 influencing colony morphology.

Previous studies have revealed intriguing observations regarding colony morphology of *E. coli* cells expressing Ag43 (6,7). The expression of Ag43 was found to result in a colony morphology described as rough or 'frizzy' (7). Mutations generated in the hydrophilic region of the N-terminal one-third of the passenger domain resulted in a loss of aggregation but did not lead to a loss of the unique morphology, rather variations in the frizzy appearance. Interestingly, these variations did not directly correlate with the aggregative capability of the mutants, suggesting that the presence of Ag43 on the cell surface impacts overall colony morphology. We hypothesize that deleting the C-terminal two-thirds of the Ag43 passenger domain in *E. coli* DH5α will result in a loss of the rough colony phenotype, characterized by round, glossy colonies. This study aims to identify the specific region within Ag43 influencing colony morphology and contribute to a deeper understanding of the functional significance of its various domains.

METHODS AND MATERIALS

Bacterial strains and growth conditions. *E. coli* DH5α (ThermoFisher) were cultured at 37°C on Luria broth or agar supplemented with 100 µg/mL of ampicillin and 1g/L of L-glucose or 2g/L of L-arabinose.

Primer design. Primers for Q5 site directed mutagenesis were designed using SnapGene to delete the C-terminal two-thirds of the passenger domain of Ag43. The pBAD-Ag43 plasmid sequence was retrieved from Addgene and the nucleotide sequence for the passenger domain was determined using UniProt. The target region was chosen based on the study performed by Klemm *et al.*, showing that insertion mutations in hydrophilic regions from amino acid position 148 to 425 showed no changes to aggregation ability of the cells expressing Ag43 but caused minor changes to colony morphology (6)**.** Primers for deletion were designed with considerations of amino acid 141 onwards until amino acid 551 (end of passenger domain) and lengths ranging from 18 to 24 nucleotides while aiming for a GC content between 40-60%. Primer pairs were selected considering differences in annealing temperatures (T_m) no greater than 4°C, avoiding significant secondary structures and ensuring specificity to the target region.
Forward primer: 5'-CCCACGAATGTCACTCTCGCC-3'
T_m = 61°C, 21bp, 62% GC.
Reverse primer: 5'-CGCCCCGGTATTAACAACGGTATC-3'
T_m = 61°C, 24bp, 54% GC.
Primers were manufactured by Integrated DNA Technologies (IDT).

Transformation of *E. coli* DH5α cells. Competent *E. coli* DH5α cells (ThermoFisher) were transformed with either pBAD24, pBAD-Ag43 (Addgene), or pSMAK plasmids. A heat-shock protocol was employed, following the methods described by Chang *et al.* (8). The plasmids were added to competent cells, followed by a 30-minute incubation on ice, 30-second heat treatment at 42°C, and a second 2-minute incubation on ice. The transformed cells were incubated at 37°C, 200 rpm for 1 hour in LB broth and selected for on LB agar plates containing ampicillin. The plates were incubated at 37°C overnight and removed from the incubator the following morning to inspect for transformed colonies.

Plasmid extraction. pBAD24, pBAD-Ag43, and pSMAK plasmids were extracted from their respective *E. coli* DH5α overnight cultures using the EZ-10 Spin Column Plasmid DNA Miniprep Kit (Bio Basic) according to manufacturer's instructions. Plasmid purity and yield was determined using NanoDrop 2000 (ThermoFisher) and stored at -20°C.

Q5 site-directed mutagenesis. The New England BioLabs Q5® Site-Directed Mutagenesis Kit (E0554) was employed to achieve a targeted deletion in the latter two-thirds of the Ag43 passenger domain (amino acids 193-552). Following the Q5 Exponential Amplification reaction, the samples were treated with the HinCII restriction enzyme (NEB) following the NEBcloner protocol. The digested samples were loaded with 6X orange loading dye

(Thermofisher) and run on a 1% agarose gel with SYBR Safe DNA Gel Stain (Thermofisher) to verify the deletion. The gel was imaged using the Bio-Rad ChemiDoc Imaging System, followed with the KLD treatment on the amplified samples. The mutant plasmid was transformed into NEB® 5-alpha Competent *E. coli* (High Efficiency) cells. Transformed cells were selected for on LB agar plates supplemented with 100 µg/mL of ampicillin.

To confirm the deletion, pSMAK was extracted from transformed cells and treated with HinCII restriction enzyme (NEB). Digested pSMAK was compared to pBAD-Ag43 treated with or without HinCII on a 1% agarose gel.

Plasmidsaurus was used to sequence a putative pSMAK plasmid sample. Sequencing results were analyzed using SnapGene and EMBOSS Water to align the sequences. Nucleotide and amino acid sequences were aligned to determine the exact nucleotides and amino acids deleted.

Glucose/Arabinose Assay. To observe Ag43 expression, aggregation, and colony morphology, cells were grown in three conditions: Luria broth (LB) only or LB supplemented with either glucose or L-arabinose. All media conditions were supplemented with 100 µg/mL of ampicillin. Glucose served as a control to suppress Ag43 expression under the pBAD vector, and L-arabinose induced the expression of Ag43 via the araBAD promoter. In solid agar plates, transformed *E. coli* DH5α cells with pBAD24, pBAD-Ag43, or pSMAK were cultured overnight at 37°C for 12-16 hours. Overnight liquid cultures were prepared by inoculating transformed cells under the same media conditions as the solid agar portion of the assay. All cultures were placed in a 37°C incubator with continuous shaking at 200 rpm. Colonies growing on solid agar were observed using a stereo microscope (Meiji). Images were captured using an iPhone 12 (Apple).

Aggregation assay. The aggregation assay was adapted from Klemm *et al.* (6). *E. coli* DH5α cells transformed with either pBAD24, pBAD-Ag43, or pSMAK were grown overnight at 37°C, 200 rpm in various liquid media conditions (LB only or LB with either glucose or L-arabinose) supplemented with 100 µg/mL ampicillin. The cultures were removed from the incubator, vortexed vigorously, and the optical density at 600 nm (OD_{600}) was measured and normalized to OD_{600} = 1.0. The turbidity of each culture was measured using the BioTek Epoch Microplate Spectrophotometer every 5 minutes for 30 minutes, and then every 10 minutes until 50 minutes by removing 100 µL from the top of each culture. Cultures were maintained at room temperature.

Western Blot. SDS-PAGE gels were prepared using the TGX Stain-Free FastCast Acrylamide Kit, 10% (Bio-Rad). 2x Laemmli Sample Buffer was prepared by mixing 2x Laemmli Sample Buffer (Bio-Rad) with beta-mercaptoethanol (BME) at a 10:1 ratio. Overnight cultures were vortexed, centrifuged, and resuspended in 2x Laemmli Sample Buffer at a 1:1 ratio. Samples were then heated to 95°C for 5 minutes before loading onto SDS-PAGE gel. Samples were stacked by running at 100V for 10 minutes and resolved by running at 200V for 1 hour. Western transfer was done onto a PVDF membrane at 25V for 1 hour. Protein transfer was confirmed with Ponceau S staining before washing with TBS-T, then blocking for 1 hour at room temperature with TBS-T in 5% Skim milk. TBS-T was used to wash the membrane between incubation steps. Anti-Ag43 primary antibody was prepared at 1:2000 dilution in TBS-T and membrane as incubated overnight at 4°C (Cusabio). StarBright Blue 700 Fluorescent secondary antibody at 1:5000 dilution in TBS-T and incubated covered for 1 hour at room temperature (Bio-Rad). The membrane was washed with TBS-T before imaging using the StarBright B700 setting on Bio-Rad ChemiDoc.

The second Western blot was performed with some modifications. Mini-PROTEAN TGX Stain-Free Precast Gels (Bio-Rad) were used in place of preparing the SDS-PAGE gels with the FastCast Kit. Western transfer was also done using the Bio-Rad Trans-Blot Turbo Transfer System onto Trans-Blot Turbo Mini PVDF Transfer Packs. The MIXED MW turbo setting was used and transferred at 25V for 7 minutes.

RESULTS

In-frame deletion of the C-terminal two-thirds of the Ag43 alpha domain was achieved using site-directed mutagenesis. Klemm *et al*. previously investigated the impact of the N-terminal one-third of the alpha domain of Ag43 on aggregation and morphology (6). To further study the morphological impact of Ag43, we generated a deletion in the C-terminal two-thirds of the alpha domain using site-directed mutagenesis. We used SnapGene to design forward and reverse primers for site-directed mutagenesis (Fig. 1A, Supplementary Figure S2A). To validate this deletion, we performed a restriction digest on the putative mutated plasmid, named pSMAK, using the HinCII restriction enzyme. We expected HinCII to linearize pBAD-Ag43, the wildtype plasmid, but leave pSMAK circularized since the deletion removed the restriction site. Gel electrophoresis confirmed this deletion (Supplementary Figure S1), and pSMAK was sent to Plasmidsaurus for sequencing. The pSMAK sequence was aligned with the pBAD-Ag43 sequence using SnapGene and EMBOSS Water, revealing that we had generated an in-frame deletion of the C-terminal two-thirds of the alpha domain. Amino acids 193-551 were deleted in pSMAK, with an intact autochaperone region (Fig. 1C, Supplementary Figure S2B). AlphaFold and ChimeraX visualized the specific region of the 3D structure of Ag43 that was deleted (Fig. 1D), providing insight into downstream predictions and analyses.

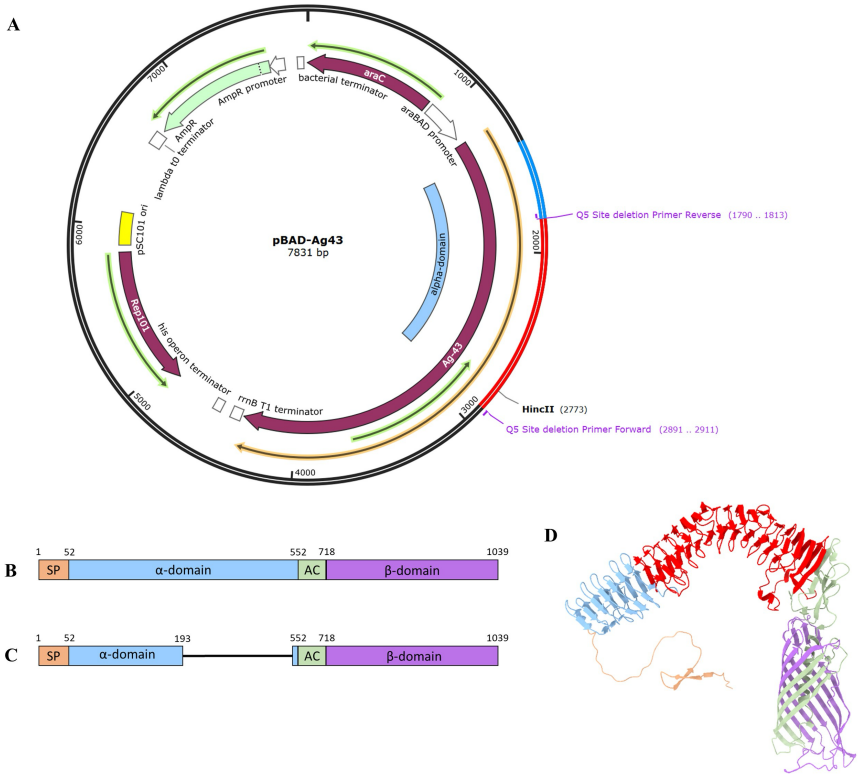

FIG. 1 In-frame deletion of the C-terminal two-thirds of the Ag43 alpha domain was achieved using site-directed mutagenesis. (A) SnapGene schematic of pBAD-Ag43 displaying the location of the forward and reverse primers for site-directed mutagenesis. The alpha domain (blue) contains a HinCII restriction site within the deleted region (red). (B) Ag43 is composed of a signal peptide (orange), alpha domain (blue), autochaperone (green), and beta domain (purple). (C) Amino acids 193-551 in the C-terminal two-thirds of Ag43 were deleted. (D) AlphaFold model of Ag43, highlighting the deleted region (red). Colours of the structure correspond to (B).

Deletion of C-terminal two-thirds of the passenger domain of Ag43 affected colony morphology and aggregation kinetics. In pBAD-Ag43 constructs, expression of wildtype *agn43* is tightly regulated by the arabinose-inducible araBAD promoter (12). Under arabinose media conditions, pBAD-Ag43 is expected to express its characteristic phenotypes: frizzy morphology in solid media and aggregation in liquid media. To study changes in morphological and aggregative properties induced by deletion of the C-terminal two-thirds of the passenger domain, we performed a solid and liquid media assay as well as an autoaggregation assay (Fig. 2). *E. coli* DH5α cells were transformed with three different plasmids: pBAD24 (empty vector), pBAD-Ag43 encoding wildtype Ag43 (WT) and pSMAK ($Ag43\Delta_{(193\text{-}551)}$). For the solid assay, we plated pBAD24, wildtype, and $Ag43\Delta_{(193\text{-}551)}$ cultures on three different agar media conditions: 1) Luria broth only (LB only negative control), 2) LB supplemented with glucose (negative control) or 3) LB supplemented with L-arabinose. Under arabinose conditions both wildtype and $Ag43\Delta_{(193\text{-}551)}$ expressed a frizzy colony morphology. However, $Ag43\Delta_{(193\text{-}551)}$ colonies had a smoother appearance compared to

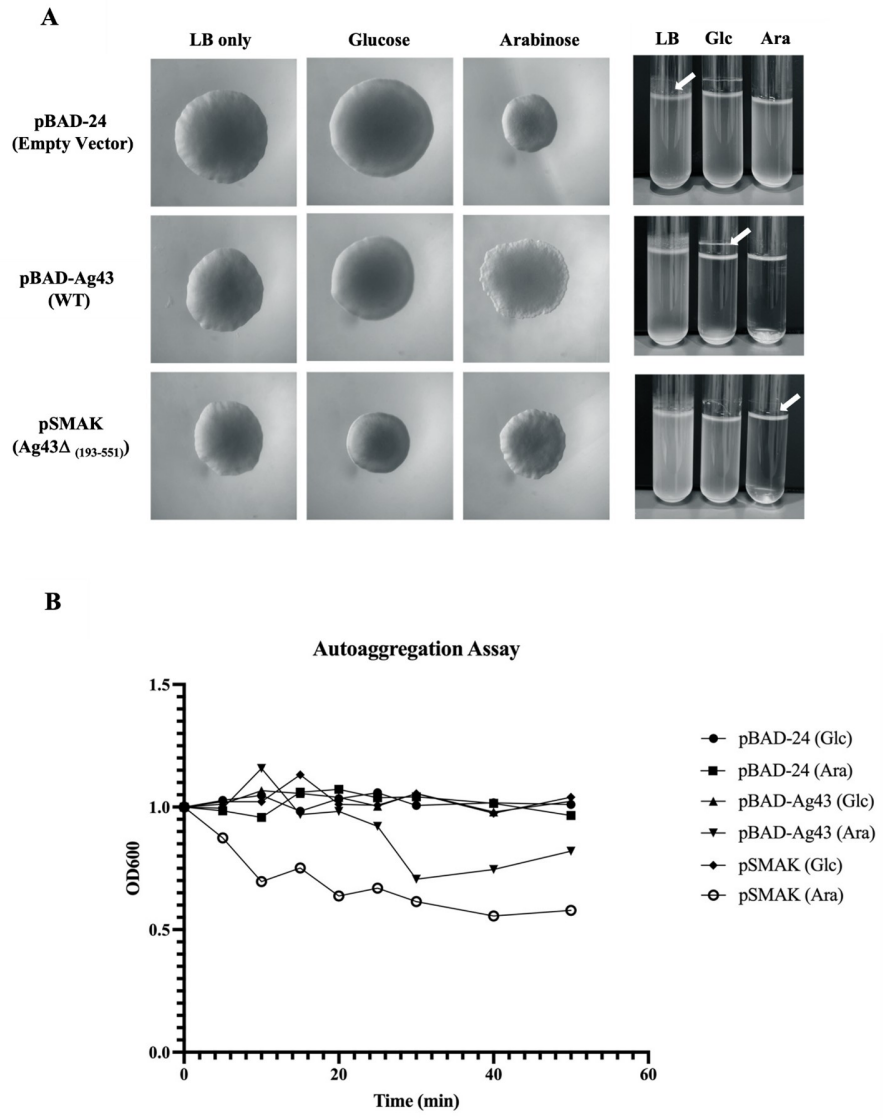

FIG. 2 Deletion of C-terminal two-thirds of the passenger domain of Ag43 affected colony morphology and aggregation kinetics. *E. coli* DH5α cells were transformed with pBAD-24 (empty vector), pBAD-Ag43 (WT) or pSMAK (Ag43Δ$_{(193-551)}$), plated and cultured on Luria (LB only), glucose or arabinose supplemented media and incubated overnight at 37°C. (A) Solid media assay showing colony morphology empty vector control, pBAD-Ag43 and pSMAK under three media conditions. WT and Ag43Δ$_{(193-551)}$ show frizzy morphology under arabinose condition. Colonies under other conditions remained smooth. Images captured at 4x magnification. (B) Liquid media assay assessing Ag43 expression by aggregation of cells. WT and Ag43Δ$_{(193-551)}$ aggregated with different kinetics. Formation of a pellicle observed in all culture media conditions. (C) Overnight liquid cultures were re-suspended, and their optical density (OD) was standardized to a value of 1. The aggregation rate was evaluated through periodic OD_{600} measurements taken every 5 minutes for the initial 30 minutes, followed by measurements every 10 minutes thereafter. Both pBAD-Ag43 and pSMAK exhibited aggregative tendencies, with pSMAK demonstrating a faster aggregation rate compared to pBAD-Ag43.

wildtype-expressing colonies. LB only and glucose media conditions across all colonies of transformed cells exhibited the expected smooth colony morphology (Fig. 2A, left). For the liquid assay, cultures for each of the transformed *E. coli* cells were set up and incubated overnight. We observed aggregation in both wildtype and Ag43Δ$_{(193-551)}$ under arabinose conditions. However, the culture containing Ag43Δ$_{(193-551)}$ had higher turbidity than that observed in the wildtype. Additionally, while cells aggregated at the bottom of the tubes in both cases the pattern of aggregation was slightly different. WT cells aggregated like a pellet while Ag43Δ$_{(193-551)}$ cells appeared like a smear surrounding the bottom. Unexpectedly, we observed a certain degree of aggregation under glucose conditions in both WT and Ag43Δ$_{(193-551)}$. The Ag43Δ$_{(193-551)}$ strain expressed greater turbidity than the WT under glucose conditions. None of the transformed cell types aggregated under LB only media conditions (Fig. 2A, right).

In the autoaggregation assay we observed aggregation kinetics of WT and Ag43Δ$_{(193-551)}$ throughout LB only, glucose supplemented, or arabinose supplemented media conditions. We resuspended overnight cultures used for the liquid assay and standardized their optical density to a value of 1. Then we proceeded to take OD_{600} measurements every 5 minutes for the first 30 minutes and every 10 minutes to a total of 50 minutes. Aligning with liquid aggregation assay results, under arabinose media conditions both WT and Ag43Δ$_{(193-551)}$ showed an aggregative trend with a progressive decrease in OD_{600} measurements. However, the Ag43Δ$_{(193-551)}$ aggregation rate was much faster than that of WT under arabinose conditions.

Under the other cell and media conditions, the aggregation rate remained stable with little variation from baseline measurements (Fig 2 B).

Lastly, in LB only, glucose or arabinose supplemented media conditions we noted the formation of a pellicle that varied in thickness based on media conditions, with LB only being the thickest and only being slightly perceptible under arabinose (Fig. 2B, white arrows). Altogether, these results suggest that deletion of C-terminal two-thirds of the passenger domain of Ag43 does not completely impair induction of frizzy colony morphology and aggregative properties.

Ag43 expression is more tightly regulated in mutant cells compared to wildtype. In addition to our previous assays, we needed further indication of the expression levels of Ag43 autotransporter in glucose and arabinose conditions. To measure protein expression, a western blot using a primary antibody binding to Ag43 was ran with whole cell lysates. Cell lysates were produced from overnight cultures of pBAD24, WT, and Ag43$\Delta_{(193\text{-}551)}$ expressing cells in LB supplemented with glucose or arabinose and grown at 37°C. Samples were loaded and ran through an SDS-PAGE gel before being transferred to a PVDF membrane and incubated with a primary antibody probing for Ag43. Signal detection was achieved with StarBright Blue 700 Secondary Antibody creating fluorescent signals corresponding to the molecular weight where Ag43 is present in our cell lysates. To determine background signals and ensure we had a proper signal specifying for Ag43, we ran lysates expressing an empty vector alongside both Ag43-expressing samples. Ag43 is expected to have a molecular weight of about 50kDa (14). Figure 3 shows the expression of Ag43 in our cell lysates under their corresponding conditions. Marker A shows our WT whole lysate signals corresponding to Ag43, which is also shown in our Ag43$\Delta_{(193\text{-}551)}$ lysate just 10 kDa lower than WT (marker B). The lower molecular weight of Ag43$\Delta_{(193\text{-}551)}$ confirms the deletion of our mutant Ag43

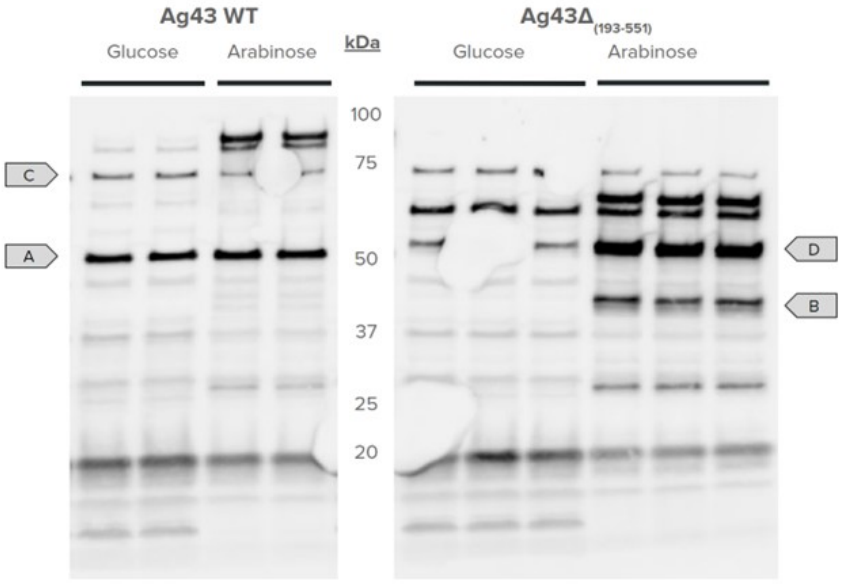

FIG. 3 Ag43 expression is more tightly regulated in mutant cells compared to wildtype. Western blot using anti-Ag43 antibody shows Ag43 detection in whole cell lysate of cells grown in arabinose or glucose conditions. (A) Surface expressed WT Ag43 observed at 50 kDa, demonstrated similar levels of expression in both glucose and arabinose conditions. B) Mutated Ag43 expression at approximately 40 kDa due to the deletion mutation resulting in a lower molecular weight compared to WT. Mutant Ag43 also expressed in arabinose but absent in glucose conditions. (C/D) Higher molecular weight Ag43 bands with similar expression patterns in both WT and mutant Ag43, where mutant cells have increased Ag43 signal intensity compared to WT.

protein. Additionally, in marker A we can identify that Ag43 is being expressed in both glucose and arabinose conditions. This coincides with our liquid assay results from Figure 2B, where there is still aggregation present, albeit slightly less in glucose conditions compared to arabinose. Marker B shows expression of Ag43$\Delta_{(193\text{-}551)}$ at a lower molecular weight compared to the WT. Ag43 is clearly expressed in arabinose conditions; however, cells grown in glucose supplemented media do not show any expression of Ag43 at the same molecular weight. This expression pattern is also reflected in the liquid culture aggregation in Figure 2B. Heavier and possibly unprocessed Ag43 signals with similar expression patterns appear on markers C and D. These signals are most intense directly above Ag43 in Ag43$\Delta_{(193\text{-}551)}$ cells in arabinose culture when compared to WT. Arabinose also seems to induce expression of double bands approximately 30 kDa above Ag43 in both Ag43$\Delta_{(193\text{-}551)}$ and WT cells. Overall, these results suggest that Ag43 expression is more tightly regulated in Ag43$\Delta_{(193\text{-}551)}$ cells compared to WT.

DISCUSSION

Ag43, a prominent member of the self-associating autotransporter (SAAT) subgroup of autotransporters (ATs), is a key player in bacterial aggregation and biofilm formation (6). These processes are vital for bacterial resilience against environmental stressors and contribute significantly to antibiotic resistance and chronic infections. Ag43 is well studied in *E. coli*, being expressed in both commensal and pathogenic strains, including uropathogenic *E. coli* (UPEC). In the case of UPEC, Ag43 is involved in disease pathogenesis by facilitating bacterial aggregation, biofilm growth, and persistence in the urinary tract. Thus, Ag43 serves as a model adhesin for investigating bacterial aggregation and biofilm production (7). The structural composition of Ag43 includes a signal peptide, alpha domain, autotransporter, and beta domain (7). Extensive research has delved into the role of the alpha domain in aggregation since its discovery in the late 20th century. However, its influence on colony morphology remains poorly understood. This study aims to fill this knowledge gap by investigating the specific role of the alpha domain in colony morphology, as colonies expressing Ag43 exhibit a distinct 'frizzy' appearance (5). To address this gap, we implemented a site-directed mutagenesis protocol, specifically targeting the deletion of the C-terminal two-thirds of the alpha domain (Fig. 1). Following this deletion, an arabinose assay was conducted in both solid and liquid media.

In the solid assay, *E. coli* DH5α cells were plated on various agar media conditions. Under arabinose conditions, both Ag43 and $Ag43_{\Delta(193\text{-}551)}$ displayed a frizzy colony morphology, but $Ag43_{\Delta(193\text{-}551)}$ exhibited a reduced frizzy morphology compared to the wildtype (Fig. 2A). In the liquid assay, $Ag43_{\Delta(193\text{-}551)}$ retained the ability to aggregate in culture (Fig. 2A). These aggregation findings align with a prior study emphasizing the critical role of the N-terminal one-third of the alpha domain in intercellular interactions involving ionic residues (7). However, recent insights into the three-dimensional structure of the alpha domain of Ag43 unveiled a right-handed, three-stranded β-helix, forming an L-shaped protein (5). This distinctive conformation, characterized by a twisted and irregular structure with the long arm of the L over its axis, constitutes a solenoid-like morphology crucial for the protein's aggregation function through hydrogen bonds and salt bridges. Previous evidence indicated that deletions in specific alpha domain regions altering the L-shape led to a complete loss of aggregation, including the removal of two β-hairpins (amino acids 268-284 and amino acids 341-357).

In contrast to these findings, our study reveals that deletion of amino acids 193-551 still resulted in aggregation (Fig. 2A). Structural and functional data by Heras *et al.* suggest that alpha domains from adjacent cells interact in a head-to-tail conformation (5). This interaction mechanism is likened to a modified molecular Velcro, where interacting bacterial surfaces, covered with hook-like AT structures, self-assemble via a "handshake" mechanism to form aggregated communities. In addition, it has been proposed that the L shape of the alpha domain strengthens its "foundations" by increasing the contact surface and the number of interactions between the alpha and beta domains, enhancing attachment to the cell surface (7). These previous findings highlight the significance of the L-shape in aggregation. However, the deletion we generated consistently resulted in aggregation in arabinose induced conditions (Fig. 2A). This suggests that the autochaperone remained intact, permitting the alpha domain to reach the extracellular space and fold, causing aggregation. While the β-hairpins may have been crucial for aggregation, it is possible this deletion altered the folding. Thus, the structure of $Ag43_{\Delta(193\text{-}551)}$, restores its aggregative abilities by modifying the alpha domain from an L-shape to a stick-like structure that allows the alpha domains on adjacent cells to interact (Fig. 4).

The necessity of the L-shaped structure in the alpha domain for Ag43-associated aggregation has been demonstrated through laboratory-induced or naturally acquired mutations. However, it is possible that Ag43 might retain its aggregative properties even in the absence of the L-shaped structure. Despite the uniqueness of the L-shaped configuration to Ag43, not all bacterial adhesins utilize this structure. Some bacterial adhesins involved in host cell attachment, such as UpaB and pertactin P.69, are capable of aggregating without relying on the L-shaped structure (14). Therefore, Ag43 aggregation following the deletion of the C-terminal two-thirds of the alpha domain suggests that such aggregative behavior may

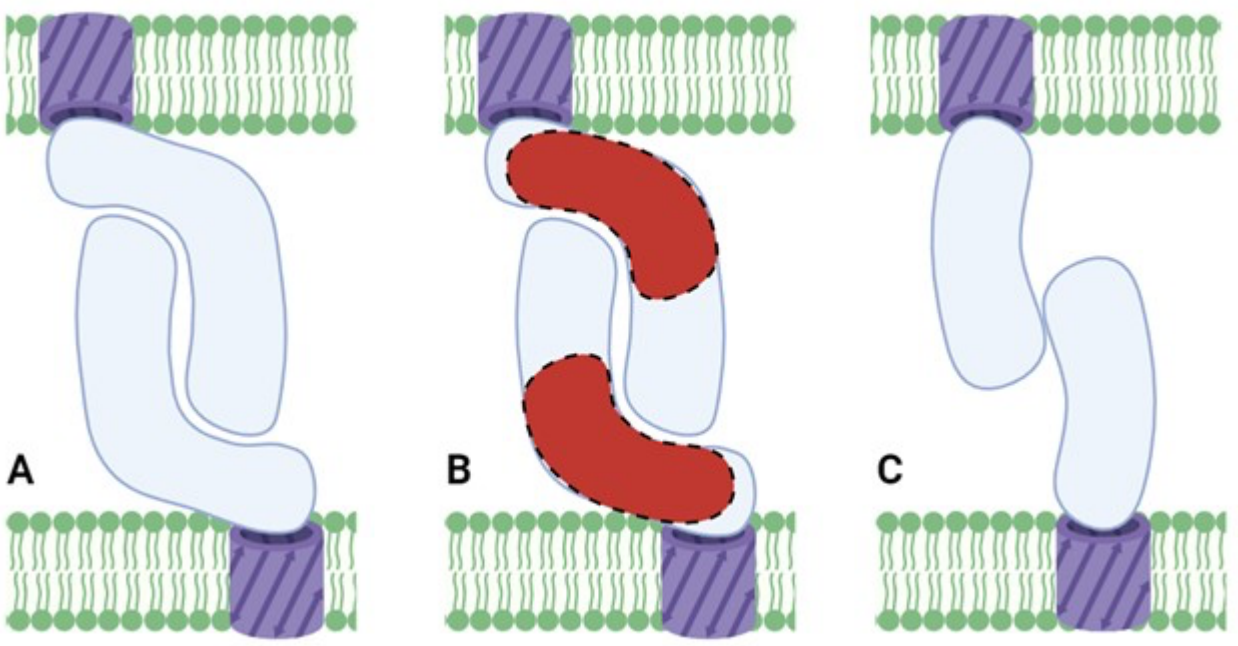

FIG. 4 Proposed Model for the Aggregating Mechanisms of Mutant Ag43Δ$_{(193-551)}$. Graphical representation of (A) Wild-type Ag43 and (B) the region targeted by Q5 deletion on the wild-type Ag43 passenger domain. (C) Represents visualization of mutant Ag43Δ$_{(193-551)}$ expressed on the surface membrane of *E. coli* while interacting with a complement Ag43 protein from another cell (13). Beta transmembrane domains are represented in purple and the alpha passenger protein is represented in light blue.

not be exclusively tied to the presence of the L-shaped structure and may manifest through alternative mechanisms.

However, it should be noted that aggregation in wildtype Ag43 appeared differently than in Ag43$_{\Delta(193-551)}$. While cells expressing WT Ag43 aggregated and settled as a precipitate-like substance, Ag43$_{\Delta(193-551)}$ aggregation appeared as a thin smear of cells along the bottom of the tube. Perhaps this model of Ag43 structure permits aggregation but alters the physical interaction between the alpha domains of neighbouring cells, modifying the aggregation phenotype. The reduced size of Ag43$_{\Delta(193-551)}$ (Fig.3) may increase the likelihood of alpha domains of neighboring cells interacting due to reduced bulk and steric hindrance. However, these interactions may not be as stable as those involved in the Velcro mechanism, leading to less long-term binding and ultimately less overall aggregation.

To further analyze the aggregation observed in Ag43$_{\Delta(193-551)}$, we performed an aggregation assay by measuring the decrease in OD$_{600}$ of *E. coli* DH5α cells expressing either Ag43 or Ag43$_{\Delta(193-551)}$. Cells were cultured in glucose or arabinose-induced conditions to observe aggregation kinetics (Fig. 2B). A decrease in OD$_{600}$ in both Ag43 and Ag43$_{\Delta(193-551)}$ under arabinose-induced conditions was observed. The trend exhibited by Ag43 is consistent with previous studies, although we did not observe a drastic decrease in comparison (5, 14). Surprisingly, OD$_{600}$ for Ag43$_{\Delta(193-551)}$ decreased at a quicker rate in comparison to that of wildtype Ag43. Perhaps, strong non-covalent interactions between alpha domains in wildtype Ag43, require more time to interact than in Ag43$_{\Delta(193-551)}$ (14). Since aggregation occurs without the full alpha domain, Ag43$_{\Delta(193-551)}$ is likely quicker at interacting with alpha domains on neighbouring cells, resulting a greater aggregation rate. However, it should be noted that this assay was performed at room temperature instead of on ice, which may explain the discrepancy observed between Ag43 and Ag43$_{\Delta(193-551)}$.

Limitations One of the limitations we encountered in our work impacted protein gel analysis. When running Western blot protein analysis assay, we used whole cell lysates instead of isolating the specific protein we are observing in the cells. The combination of using whole cell lysates paired with polyclonal primary antibody resulted in signals from unidentified regions excluding the expected Ag43 (Fig.3 C/D). These regions could possibly be Ag43

segments from the whole cell lysate or non-specific binding though of our primary antibody, which could be clarified if we had performed a mild heat treatment to the cells to release the alpha domain of Ag43 which then would have given us only the Ag43 protein and no intracellular components that detract from our signal (7). Additional control measures by re-probing our Western blots for housekeeping proteins to normalize protein expression may have given us insight into the comparability of wildtype Ag43 and $Ag43_{\Delta(193\text{-}551)}$. Finally, time was another limitation regarding our aggregation assay, which could have been improved by keeping aggregating cell cultures on ice to have more consistent measurements. With longer timepoints and slower aggregation from icing our cell cultures, we could have accurate and improved comparisons between the speed and efficiency of aggregation between samples.

Conclusions Site directed mutagenesis facilitated an in-frame deletion of the C-terminal two-thirds of the alpha domain of Ag43, creating pSMAK, a construct that was confirmed by whole plasmid sequencing. Assays in various media conditions provided nuanced insights into the phenotypic behavior of WT and $Ag43\Delta_{(193\text{-}551)}$ cells. In liquid culture, WT cells demonstrated aggregation in both arabinose and glucose conditions. However, arabinose induced more aggregation compared to glucose. In contrast, $Ag43\Delta_{(193\text{-}551)}$ cells exhibited differential behavior, aggregating exclusively in arabinose conditions, and showing reduced aggregation in glucose. On LB agar, 'frizzy' and smooth colony morphologies were observed in arabinose and glucose conditions respectively. The deletion generated in pSMAK did not result in smooth colony morphology as initially hypothesized. Notably, $Ag43_{\Delta(193\text{-}551)}$ exhibited altered behavior compared to the wild type under glucose and arabinose conditions, emphasizing the potential functional impact of this specific deletion. This intricacy in the interplay between the Ag43 protein and environmental conditions opens avenues for further exploration into the specific functional consequences of the deletion and its implications for the behavior of *E. coli* DH5α.

Future Directions In our study, which primarily focused on morphological and aggregative changes resulting from the deletion of the C-terminal two-thirds of the Ag43 alpha domain, there emerges a critical avenue for future research in the exploration of functional consequences. While our current investigation provides valuable insights into the altered appearance and aggregation kinetics, it falls short in directly addressing the functional properties of Ag43 beyond mere visual observations. To bridge this gap, future directions should include comprehensive functional assays, notably investigating adhesion capabilities and biofilm formation (15). These assays could shed light on whether the deletion influences Ag43's ability to mediate bacterial adhesion and impact biofilm structure and density. Furthermore, delving into cell interaction studies will unveil whether the deleted region plays a role in interactions with host cells, bearing implications for pathogenicity or symbiotic relationships. Comparative studies between the wildtype Ag43 and the deleted variant in various functional assays would offer a direct comparison, aiding in identifying specific changes attributable to the deletion. Additionally, employing biophysical techniques and *in vivo* models can provide quantitative insights and assess the physiological relevance of the observed changes. Considering long-term impact assessment and global profiling through transcriptomics and proteomics would further enhance our understanding of the functional implications of the C-terminal deletion in Ag43. These future avenues will contribute significantly to unraveling the biological consequences of the observed structural modification in our study.

ACKNOWLEDGEMENTS

We extend our sincere thanks to the MICB471 teaching team, including David Oliver, Herieth Ringo, and Jade Muileboom, for their invaluable guidance and unwavering support throughout our project journey. Their expertise and dedication have played a vital role in the successful completion of our objectives. Additionally, we express our appreciation to the Microbiology and Immunology Department for their generous funding and provision of essential resources, which have been instrumental in achieving our project milestones.

Finally, our gratitude extends to our fellow classmates for their collaborative efforts and support, making a significant contribution to the overall success of our work.

CONTRIBUTIONS

Manuscript. AN: Methods, Figures, Results, Discussion, References. **KM:** Methods, Figures, Results, Discussion, Limitations, Supplementary Materials. **MT:** Title, Abstract, Introduction, Methods, Discussion, Conclusion, Future Directions, Acknowledgements, References. **SZ:** Methods, Figures, Results, Discussion, Supplementary Materials.

REFERENCES

1. **Meuskens I, Saragliadis A, Leo JC, Linke D.** 2019. Type V Secretion Systems: An Overview of Passenger Domain Functions. *Front Microbiol* **10**:1163.
2. **Wallecha A, Oreh H, van der Woude MW, deHaseth PL.** 2014. Control of Gene Expression at a Bacterial Leader RNA, the agn43 Gene Encoding Outer Membrane Protein Ag43 of *Escherichia coli. J Bacteriol* **196**:2728–2735.
3. **Kjærgaard K, Schembri MA, Ramos C, Molin S, Klemm P.** 2000. Antigen 43 facilitates formation of multispecies biofilms. *Environmental Microbiology* **2**:695–702.
4. **Vaish R, Pradeep M, Setty C, Kandi V.** Evaluation of Virulence Factors and Antibiotic Sensitivity Pattern of Escherichia Coli Isolated from Extraintestinal Infections. *Cureus* **8**:e604.
5. **Heras B, Totsika M, Peters KM, Paxman JJ, Gee CL, Jarrott RJ, Perugini MA, Whitten AE, Schembri MA.** 2014. The antigen 43 structure reveals a molecular Velcro-like mechanism of autotransporter-mediated bacterial clumping. *Proc Natl Acad Sci USA* **111**:457–462.
6. **Klemm P, Hjerrild L, Gjermansen M, Schembri MA.** 2004. Structure-function analysis of the self-recognizing Antigen 43 autotransporter protein from *Escherichia coli. Molecular Microbiology* **51**:283–296.
7. **van der Woude MW, Henderson IR.** 2008. Regulation and Function of Ag43 (Flu). *Annu Rev Microbiol* **62**:153–169.
8. **Chang AY, Chau VY, Landas JA, Pang Y.** 2017. Preparation of calcium competent *Escherichia coli* and heat-shock transformation. *JEMI Methods* **1**:22-25.
9. **Biolabs NE.** Quick Protocol for Q5® Site-Directed Mutagenesis Kit (E0554). *NEB.*
10. Flu antibody. *Cusabio Life Science* – Your Biology Science Partner.
11. Starbright Blue 700 fluorescent secondary antibodies. *BioRad.*
12. **Schembri MA, Hjerrild L, Gjermansen M, Klemm P.** 2003. Differential Expression of the *Escherichia coli* Autoaggregation Factor Antigen 43. *J Bacteriol* **185**:2236–2242.
13. Scientific Image and Illustration Software. BioRender.
14. **Vo JL, Ortiz GCM, Totsika M, Lo AW, Hancock SJ, Whitten AE, Hor L, Peters KM, Ageorges V, Caccia N, Desvaux M, Schembri MA, Paxman JJ, Heras B.** 2022. Variation of Antigen 43 self-association modulates bacterial compacting within aggregates and biofilms. *npj Biofilms Microbiomes* **8**:20.
15. **Ulett GC, Valle J, Beloin C, Sherlock O, Ghigo J-M, Schembri MA.** 2007. Functional Analysis of Antigen 43 in Uropathogenic *Escherichia coli* Reveals a Role in Long-Term Persistence in the Urinary Tract. *Infect Immun* **75**:3233–3244.